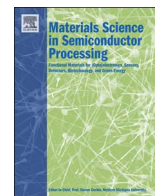




ELSEVIER

Contents lists available at ScienceDirect

Materials Science in Semiconductor Processing

journal homepage: www.elsevier.com/locate/mssp

Formation and characterization of $\text{Ge}_{1-x-y}\text{Si}_x\text{Sn}_y/\text{Ge}_{1-x}\text{Sn}_x/\text{Ge}_{1-x-y}\text{Si}_x\text{Sn}_y$ double heterostructures with strain-controlled $\text{Ge}_{1-x-y}\text{Si}_x\text{Sn}_y$ layers

Masahiro Fukuda^{a,*}, Takashi Yamaha^{a,b}, Takanori Asano^{a,b}, Syunsuke Fujinami^a, Yosuke Shimura^{a,1}, Masashi Kurosawa^{a,c}, Osamu Nakatsuka^a, Shigeaki Zaima^{a,c}

^a Department of Crystalline Materials Science, Graduate School of Engineering, Nagoya University, Furo-cho, Chikusa-ku, Nagoya 464-8603, Japan

^b The Japan Society for the Promotion of Science, Research Fellow, 5-3-1 Kojimachi, Chiyoda-ku, Tokyo 102-0083, Japan

^c Institute of Materials and Systems for Sustainability, Nagoya University, Furo-cho, Chikusa-ku, Nagoya 464-8603, Japan

ARTICLE INFO

Keywords:

Germanium silicon tin
Ternary alloy
Strain
Heterostructure
Epitaxy
Group-IV semiconductor

ABSTRACT

The formation of $\text{Ge}_{1-x-y}\text{Si}_x\text{Sn}_y/\text{Ge}_{1-x}\text{Sn}_x/\text{Ge}_{1-x-y}\text{Si}_x\text{Sn}_y$ double heterostructures with strain-controlled $\text{Ge}_{1-x-y}\text{Si}_x\text{Sn}_y$ layers and their crystalline properties were investigated. We achieved the epitaxial growth of double heterostructures consisting of a $\text{Ge}_{1-x}\text{Sn}_x$ layer with a Sn content of 9% sandwiched between compressive- or tensile-strained $\text{Ge}_{1-x-y}\text{Si}_x\text{Sn}_y$ layers. The strain sign of the $\text{Ge}_{1-x-y}\text{Si}_x\text{Sn}_y$ epitaxial layer influenced the crystallinity of the double heterostructures. Compressive-strained $\text{Ge}_{1-x-y}\text{Si}_x\text{Sn}_y$ layers provided double heterostructures with higher crystallinity than the tensile-strained ones. The magnitude of strain in the $\text{Ge}_{1-x-y}\text{Si}_x\text{Sn}_y$ layers also affected the surface roughness of the double heterostructures. Low surface roughness was achieved by decreasing the magnitude of strain in the $\text{Ge}_{1-x-y}\text{Si}_x\text{Sn}_y$ layers. Moreover, the strain sign and/or Si content in $\text{Ge}_{1-x-y}\text{Si}_x\text{Sn}_y$ influenced the thermal stability of the double heterostructures. Compressive-strained $\text{Ge}_{1-x-y}\text{Si}_x\text{Sn}_y$ and/or a low Si content in $\text{Ge}_{1-x-y}\text{Si}_x\text{Sn}_y$ improved the thermal stability of the double heterostructures to withstand annealing temperatures as high as 400 °C.

1. Introduction

The integration of photonic devices on silicon (Si) ultra-large-scale integrated circuit (ULSI) platforms to improve performance and realize new functions has been attracting much attention [1]. Introducing optoelectronic interconnections into Si ULSI has enabled us to lower power consumption by 30% [2]. Considering the integration of optoelectronic devices such as photodetectors, waveguides, and light emitters with Si ULSI, group-IV semiconductor materials display the advantage of good affinity with current Si LSI processes.

Recently, germanium tin ($\text{Ge}_{1-x}\text{Sn}_x$) alloys have received much interest for use in optoelectronic applications [3–6] because their indirect–direct crossover takes places at a Sn content higher than about 10% using only group-IV elements [7]. Photodetectors and waveguides with group-IV semiconductors such as Ge, $\text{Ge}_{1-x}\text{Sn}_x$ binary alloy, and $\text{Ge}_{1-x}\text{Sn}_x/\text{Ge}$ heterostructure have been reported [8–10]. In $\text{Ge}_{1-x}\text{Sn}_x$ p–i–n detector, the optical responsivity for wavelengths longer than 1.55 μm was improved by increasing the Sn content of the alloy [9]. Also, the photodetection limit has been extended to 2.2 μm in photo-

detectors using a $\text{Ge}_{1-x}\text{Sn}_x/\text{Ge}$ heterostructure [10]. A theoretical calculation has predicted that a laser diode with a $\text{Ge}_{1-x}\text{Sn}_x$ active region should achieve both a direct band gap and tuning of the mid-infrared wavelength in the range of 1.8–3.0 μm [11]. In addition, lasing from a Fabry–Perot waveguide cavity structure of $\text{Ge}_{1-x}\text{Sn}_x$ with a Sn content as high as 12.6% was reported recently [12]. At present, lasing from cavity structures of direct-bandgap $\text{Ge}_{1-x}\text{Sn}_x$ is limited to temperatures below 90 K with high-power optical pumping of over 300 kW/cm^2 . The lasing temperature of $\text{Ge}_{1-x}\text{Sn}_x$ is still below 130 K even using a microdisk structure [13]. We need to develop a carrier confinement structure for the $\text{Ge}_{1-x}\text{Sn}_x$ active layer in semiconductor lasers to raise their lasing temperature.

To realize effective carrier confinement for application in high-performance lasers, it is necessary to achieve type-I energy band alignment with band offsets sufficiently larger than $k_B T$ (k_B and T are the Boltzmann constant and temperature, respectively; 26 meV at room temperature) at both conduction and valence band edges. In a previous study of group-III–V compound semiconductor lasers such as GaInP/AlInP, lasing parameters including the low threshold current

* Corresponding author.

E-mail address: mfukuda@alice.xtal.nagoya-u.ac.jp (M. Fukuda).

¹ Present affiliation: Shizuoka University, Japan.

<http://dx.doi.org/10.1016/j.mssp.2016.10.024>

Received 28 July 2016; Received in revised form 23 September 2016; Accepted 17 October 2016

Available online xxxxx

1369-8001/© 2016 Elsevier Ltd. All rights reserved.

density and high operation temperature were improved using a carrier confinement structure [14]. Considering previous optoelectronic devices, carrier confinement is certainly an important technology to improve the performance of group-IV semiconductor lasers.

Theoretical calculations of $\text{Ge}_{1-x}\text{Sn}_x$ binary and germanium silicon tin ($\text{Ge}_{1-x-y}\text{Si}_x\text{Sn}_y$) ternary alloys have predicted that a multiple-quantum-well structure of $\text{Ge}_{0.90}\text{Sn}_{0.10}/\text{Ge}_{0.75}\text{Si}_{0.15}\text{Sn}_{0.10}$ will realize type-I energy band alignment with enough large band offsets at conduction and valence band edges [15]. This structure should raise the lasing temperature by suppressing Auger recombination. For effective carrier confinement, a $\text{Ge}/\text{Ge}_{1-x}\text{Sn}_x/\text{Ge}$ structure has been reported [16]. However, a theoretical calculation of this structure has predicted that the band offset between Ge and $\text{Ge}_{1-x}\text{Sn}_x$ was small at the conduction band edge, so effective carrier confinement has to be still developed.

Our group recently reported the formation of pseudomorphic $\text{Ge}_{1-x-y}\text{Si}_x\text{Sn}_y/\text{Ge}$ heterostructure and experimentally demonstrated that the band offset at the $\text{Ge}_{1-x-y}\text{Si}_x\text{Sn}_y/\text{Ge}$ interface can be controlled by changing Si and Sn contents [17]. We found that a $\text{Ge}_{1-x-y}\text{Si}_x\text{Sn}_y/\text{Ge}$ heterostructure with Sn and Si contents larger than 28% and 8%, respectively, realized type-I energy band alignment, which practically achieved band offsets larger than 100 meV at both conduction and valence band edges. Considering these results, a $\text{Ge}_{1-x-y}\text{Si}_x\text{Sn}_y/\text{Ge}_{1-x}\text{Sn}_x/\text{Ge}_{1-x-y}\text{Si}_x\text{Sn}_y$ double heterostructure should also show promise an effective carrier confinement structure with a type-I band alignment for light emitter and semiconductor laser diode applications using only group-IV elements.

However, there are few reports of the formation of double heterostructures using $\text{Ge}_{1-x}\text{Sn}_x$ and $\text{Ge}_{1-x-y}\text{Si}_x\text{Sn}_y$. Some crystallographic challenges need to be solved to establish the formation of heterostructures with $\text{Ge}_{1-x}\text{Sn}_x$ -related group-IV semiconductors. One is that it is difficult to increase the substitutional Sn content in $\text{Ge}_{1-x}\text{Sn}_x$ and $\text{Ge}_{1-x-y}\text{Si}_x\text{Sn}_y$ compound alloys because the thermal equilibrium solid solubility limits of Sn in Ge and Si are as low as 1% and 0.1%, respectively [18,19]. The precipitation of Sn from $\text{Ge}_{1-x}\text{Sn}_x$ -related material layers needs to be prevented during crystal growth and post processing.

In addition, it is essential to control the strain structure to form heterostructures. The influence of strain on the crystallinity of $\text{Si}_{1-x}\text{Ge}_x$ has been investigated [20], and our group previously reported the influence of strain on the crystallinity of $\text{Ge}_{1-x-y}\text{Si}_x\text{Sn}_y/\text{Ge}$ systems [21]. Considering these previous studies, we expect that the strain in a $\text{Ge}_{1-x-y}\text{Si}_x\text{Sn}_y$ epitaxial layer will strongly influence the crystallinity of double heterostructures. Therefore, the crystallinity may be improved by controlling the strain sign (compressive or tensile strain) of $\text{Ge}_{1-x-y}\text{Si}_x\text{Sn}_y$ layers. However, the influence of the strain in a $\text{Ge}_{1-x-y}\text{Si}_x\text{Sn}_y$ layer on the crystallinity of $\text{Ge}_{1-x-y}\text{Si}_x\text{Sn}_y/\text{Ge}_{1-x}\text{Sn}_x/\text{Ge}_{1-x-y}\text{Si}_x\text{Sn}_y$ double heterostructures has not been investigated in detail yet.

In this study, we examine the formation of $\text{Ge}_{1-x-y}\text{Si}_x\text{Sn}_y/\text{Ge}_{1-x}\text{Sn}_x/\text{Ge}_{1-x-y}\text{Si}_x\text{Sn}_y$ double heterostructures with strain-controlled $\text{Ge}_{1-x-y}\text{Si}_x\text{Sn}_y$ layers on Ge substrates and investigate the influence of elemental contents and strain on the crystallinity and thermal stability of the structures.

2. Experimental procedure

P-type Ge(001) wafers were used as substrates for the growth of $\text{Ge}_{1-x-y}\text{Si}_x\text{Sn}_y/\text{Ge}_{1-x}\text{Sn}_x/\text{Ge}_{1-x-y}\text{Si}_x\text{Sn}_y$ double heterostructures. After chemical cleaning in alkaline ($\text{NH}_4\text{OH}:\text{H}_2\text{O}=1:4$) and sulfuric acid ($\text{H}_2\text{SO}_4:\text{H}_2\text{O}=1:7$) solutions, substrates were thermally cleaned at 430 °C for 30 min in an ultrahigh-vacuum chamber. Then, $\text{Ge}_{1-x-y}\text{Si}_x\text{Sn}_y$ (30 nm, third layer)/ $\text{Ge}_{0.91}\text{Sn}_{0.09}$ (15 nm, second layer)/ $\text{Ge}_{1-x-y}\text{Si}_x\text{Sn}_y$ (30 nm, first layer) or Ge (30 nm, third layer)/ $\text{Ge}_{0.91}\text{Sn}_{0.09}$ (15 nm, second layer)/Ge (30 nm, first layer) layers were successively grown on substrates by molecular beam epitaxy at a base

Table 1

Elemental contents and strain values in the $\text{Ge}_{1-x-y}\text{Si}_x\text{Sn}_y$ first and third layers and $\text{Ge}_{1-x}\text{Sn}_x$ second layers.

Sample ID	Contents in GeSiSn (%)			Strain in GeSiSn (%)	Strain in GeSn (%)
	Ge	Si	Sn		
A	66	23	11	-0.69	-1.29
B	41	50	9	0.68	-1.39
C	49	42	9	0.36	-1.42
D	100	0	0	0	-1.36

pressure below 10^{-7} Pa. Ge and Sn were deposited using Knudsen cells, and Si was deposited using electron-beam evaporation. The growth rates of $\text{Ge}_{1-x-y}\text{Si}_x\text{Sn}_y$, Ge, and $\text{Ge}_{1-x}\text{Sn}_x$ were 1.0–1.3 nm/min. The growth temperature of $\text{Ge}_{1-x-y}\text{Si}_x\text{Sn}_y$ and Ge layers was 200 °C, and that of $\text{Ge}_{1-x}\text{Sn}_x$ layers was 150 °C. The elemental contents of the $\text{Ge}_{1-x-y}\text{Si}_x\text{Sn}_y$ layers in the samples are summarized in Table 1. Some samples were annealed at 300–500 °C for 10 min in dry N_2 to examine the thermal stability of the double heterostructures.

The elemental contents and strain in $\text{Ge}_{1-x-y}\text{Si}_x\text{Sn}_y$ and $\text{Ge}_{1-x}\text{Sn}_x$ epitaxial layers were evaluated using Raman spectroscopy (Nanophoton, RAMAN-11, wavelength of probe laser: 532 nm) and X-ray diffraction two-dimensional reciprocal space mapping (XRD-2DRSM) on a diffractometer (Philips, X'Pert PRO MRD) with a Cu K α X-ray source. Raman spectroscopy is an effective method to characterize $\text{Ge}_{1-x-y}\text{Si}_x\text{Sn}_y$ ternary alloy layers because both the contents and strain in $\text{Ge}_{1-x-y}\text{Si}_x\text{Sn}_y$ can be estimated. The crystalline structures of double heterostructures were characterized using in-situ reflection high-energy electron diffraction (RHEED, ANELVA), XRD-2DRSM, and atomic force microscopy (AFM; JEOL, JSPM-4200). The thermal stability of the double heterostructures was characterized using XRD 2θ - ω measurements.

3. Results and discussion

3.1. Formation of double heterostructures and crystalline properties

We observed the surface crystalline structure of each epitaxial layer during heterostructure fabrication using in-situ RHEED. In-situ RHEED observation results for sample A, B, and D after the growth of $\text{Ge}_{1-x-y}\text{Si}_x\text{Sn}_y$, $\text{Ge}_{1-x}\text{Sn}_x$, and Ge layers are presented in Fig. 1(a), (b), and (c), respectively. The incident electron beam was irradiated along the [110] direction. Streaky diffraction patterns are observed in sample D with a $\text{Ge}_{1-x}\text{Sn}_x$ layer sandwiched between Ge layers even after the growth of the Ge third layer, indicating that the epitaxial layers formed at each growth stage possessed atomically flat surfaces. Streaky and spotty patterns are observed for sample A and B, respectively, which indicates that epitaxial layers grew on Ge substrates, and only slightly rough surfaces were formed at each growth stage. We fabricated $\text{Ge}_{1-x-y}\text{Si}_x\text{Sn}_y/\text{Ge}_{1-x}\text{Sn}_x/\text{Ge}_{1-x-y}\text{Si}_x\text{Sn}_y$ double heterostructures with high Si and Sn contents of 23–50% and 9–11%, respectively. Fig. 2 shows horizontal intensity profiles across the [0 0] streak of the RHEED pattern of sample B after the growth of each layer. Weak peaks are observed at the 4/5 position after the growth of the $\text{Ge}_{1-x-y}\text{Si}_x\text{Sn}_y$ first and third layers. Superstructure (5 \times 1) has been reported for $\text{Ge}_{1-x-y}\text{Si}_x\text{Sn}_y$ on Si(100) [22] and Sn on Si(100) [23]. The weak diffraction peak observed at the 4/5 position in this study would be related to the surface reconstruction caused by Sn introduction.

Fig. 3(a) and (b) show XRD-2DRSM results around the reciprocal lattice point of $\text{Ge}224$ for sample A and B, respectively. The diffraction peaks related to the $\text{Ge}_{1-x}\text{Sn}_x$ and $\text{Ge}_{1-x-y}\text{Si}_x\text{Sn}_y$ layers are observed at the same reciprocal space (Q_x) value of the diffraction peak related to the Ge(001) substrate. This indicates that the $\text{Ge}_{1-x}\text{Sn}_x$ and $\text{Ge}_{1-x-y}\text{Si}_x\text{Sn}_y$ layers grew pseudomorphically on the Ge(001) substrate. Moreover, thickness fringes around the diffraction peaks are

Download English Version:

<https://daneshyari.com/en/article/5005896>

Download Persian Version:

<https://daneshyari.com/article/5005896>

[Daneshyari.com](https://daneshyari.com)